Modal analysis of Lamb wave generation in elastic plates by liquid wedge transducers

X. Jia
Groupe de Physique des Solides, Universités Paris 7 et Paris 6, Tour 23, 2 place Jussieu, 75251 Paris Cedex 05, France

(Received 9 May 1996; accepted for publication 17 September 1996)

A modal analysis is presented to describe the excitation of Lamb waves in an elastic plate using a liquid wedge transducer. Analytical expression for the displacement of a given mode is derived for the excitation by a uniform bounded beam. In contrast to previous studies, the contribution of the reflected wave is included in the input exciting forces using a perturbation theory. The conversion efficiency, defined as the ratio of the guided mode power to the incident power, is related to a single parameter which depends on the rate of attenuation due to leakage from the guided wave into the liquid wedge. Numerical results relevant to the fundamental Lamb modes are obtained as a function of frequency for various incident beam widths and plate thickness. Using optical interferometric detection, direct measurements of the Lamb modes displacements have been carried out in aluminium plates to verify the theoretical analysis. [S0001-4966(97)00402-5]

PACS numbers: 43.35.Pt, 43.35.Sx [HEB]

INTRODUCTION

Lamb waves propagating in an elastic plate have a great deal of interest for flaw detection and material characterization of layer structures.[1–6] Victorov[1] has reviewed in detail the use of Rayleigh and Lamb waves in nondestructive testing and monitoring applications. Also, in the past decade, there has been increasing interest in the fields of sensors that employ ultrasonic Lamb waves.[7–9]

Lamb waves can be excited and detected by a variety of methods. For signal processing applications, Lamb waves are generated by using interdigital electrodes on piezoelectric crystals or on piezoelectric films deposited on a nonpiezoelectric substrate.[7,8] In nondestructive testing, the wedge method is probably the most well known in which a prism or wedge is employed to convert bulk waves into Lamb waves.[1] Other transduction techniques have also been reported in the literature, including optical methods,[6,10,11] electromagnetic acoustic transducers (EMATs),[12] capacitance transducers, and air-coupled transducers.[13] The major advantage of the noncontact techniques lies in the elimination of the coupling materials, which is undesirable or impossible in applications such as the testing of hot metals, or structures where the surface contamination produced by a coupling fluid cannot be tolerated. Recent work using lasers for both generation and detection is potentially very attractive.[14,15] This laser ultrasonic technique has the advantage of being noncontact and scanned easily and rapidly over the surface of an object, though the required equipment is bulky and expensive and has mainly been used in the laboratory rather than in industrial testing applications. At present, in the majority of standard ultrasonic testing, piezoelectric transducers remain the most utilized for guided wave excitations, since the manufacture and use of these transducers are well understood and they are readily available.

Theoretical treatments of the excitation of Lamb and other guided waves have been reported extensively in the literature by Victorov,[1] Miklowitz,[16] Achenbach,[17] and others.[18,19] In most of these theoretical studies, the problem is generally resolved as a function of input force using integral transform techniques. For transient excitation problems, the solutions are derived by first applying the Laplace transform with respect to time and the exponential Fourier or Hankel transform with respect to space. The inverse transformation integrals are then carried out by the evaluation of residues via the method of stationary phase or by the method of generalized rays. As can be found in the literature (see Ref. 16; for example), the evaluation of these integrals in the first approach involves the understanding of the intricate behavior of the dispersion relations for real as well as complex wave numbers. The theory of generalized rays is an exact method involving dynamic Green's functions. It quickly becomes computationally intense as the number of ray paths from source to receiver becomes large. Furthermore, explicit expressions of the input forces are generally required in these formalisms for deriving displacement fields. However, this information is not always known *a priori* in practice. In the wedge method, for example, the input forces shall depend not only the incident wave but also the reflected one. This reflected wave is theoretically coupled to guided waves which are to be determined. Victorov[1] has calculated the displacement field of Lamb waves excited by a uniform bounded longitudinal beam, using the Fourier transform technique. In his analysis, the input force contributing to the wave reflection and radiation was neglected.

Normal-mode analysis offers an alternative approach for treating the problem of waveguide excitation. This approach, particularly practical and readily usable for descriptions in the far field, is widely used in electromagnetism[20] and acoustics.[21,22] The principle of the mode theory is to express the excited field as the sum of normal modes obtained in a stress-free waveguide. The contribution of each mode to the resulted fields is determined in terms of the associated power

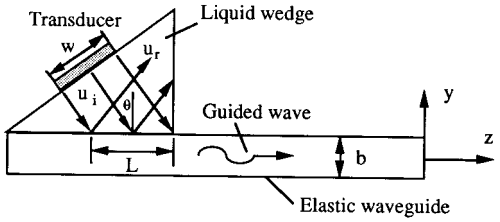

FIG. 1. Schematic diagram of Lamb wave excitation by the wedge method.

flow using the orthorgonality condition of eigenmodes. Mode theory has been successfully applied to study the excitation by the wedge method of nondispersive surface waves such as Rayleigh[23,24] and Stoneley modes.[25] Such an approach concerning the Lamb wave excitation was also reported recently, in which particular attention was focused on the angular dependence of the excitation amplitude of a given mode in the neighborhood of the Snell's law angle. Like Victorov's analysis, the influence of the wave reflection and radiation was again not considered in that work.[26]

The purpose of this paper is to present a modal analysis of the Lamb wave excitation by a liquid wedge, which takes into account the effects of wave reflection and radiation. Special attention will be concentrated on the excited displacement and conversion efficiency of a given mode as a function of the parameters of the wedge transducer and the plate waveguide. Quantitative measurements of the displacement fields using optical interferometric detection will be used to verify the theoretical prediction.

I. THEORY

In this section, we shall first describe briefly the general treatment of waveguide excitation using the mode theory. Then we will examine the input force loading introduced by the wedge coupling before developing the numerical computation for the specific case of Lamb modes.

A. General formulation of the mode theory for waveguide excitation problem

Consider a waveguide in layered geometry as shown in Fig. 1, for example, where the field quantities such as particle displacement **u** and stress **T** are assumed to be independent of the x coordinate. The resulting fields in a perturbed waveguide can be expressed by the mode expansion:

$$\mathbf{u}(y,z)=\sum_n a_n(z)\mathbf{u}_n(y), \tag{1a}$$

$$\mathbf{T}(y,z)=\sum_n a_n(z)\mathbf{T}_n(y), \tag{1b}$$

where n denotes the nth eigenmode of a stress-free waveguide and a_n is the mode amplitude. For the observation at a distance far from the source only the propagating mode is significant. To determine the amplitude coefficient of each mode $a_n(z)$, we make use of the reciprocity relation and the orthogonality condition of eigenmodes, which leads to the equation governing a mode amplitude of the excited mode,[21,22]

$$\left(\frac{d}{dz}+ik_n\right)a_n(z)=\frac{f_n(z)}{4P_n}, \tag{2}$$

where k_n is real representing the wave number of the nth propagating mode, P_n is the associated average power flow per unit width along the x direction,

$$P_n=\frac{i\omega}{4}\int_{-b/2}^{b/2}(-\mathbf{u}_n^*\cdot\mathbf{T}_n-\mathbf{u}_n\cdot\mathbf{T}_n^*)\cdot\mathbf{e}_z\,dy, \tag{3}$$

b being the thickness of the layer (e.g., elastic plate) and $\mathbf{e}_z$ the unit vector along the z direction. Here f_n is the input loading applied across the layer,

$$f_n(z)=i\omega\int_{-b/2}^{b/2}\mathbf{u}_n^*(y)\cdot\mathbf{F}(y,z)dy. \tag{4}$$

B. Excitation of guided modes by a liquid wedge

The principle of the wedge method can be understood by a mode conversion process shown in Fig. 1. When a plane wave is incident on the guide at the angle defined by the Snell law $\sin\theta_n=c_0/v_n$, where c_0 is the sound velocity in the liquid wedge and v_n is the phase velocity of a guided mode, a part of the wave is reflected directly and the rest is to excite the given mode in the layer. In practice, the width of the incident beam is not infinite but several times larger than the acoustic wavelength. Generally speaking, the wider the wave beam is, the narrower the angular range allowed for exciting the given wave.[1,26] The distribution of the exciting forces resulting from both the incident and reflected waves are located on the surface of the guide ($y=b/2$) within a length L under the wedge transducer along the z axis and with a width d along the x axis. As a result, the input force function of Eq. (4) takes the form

$$f_n(z)=i\omega[\mathbf{u}_n^*(y)\cdot\mathbf{T}(y,z)\cdot\mathbf{e}_y]_{y=b/2}. \tag{5}$$

In the case where the wedge is a nonviscous liquid, only normal stress T_{yy} is transferred onto the surface of the guide. Assuming the particle displacements u_i and u_r associated with incident and reflected waves, respectively, the boundary conditions to be satisfied at the surface, $y=b/2$, can be written as

$$(-u_i+u_r)\cos\,\theta_n=a_nu_{ny}(y=b/2) \tag{6a}$$

for the normal component of the particle displacement and

$$T_{yy}(y=b/2,z)=-i\omega Z_0(u_i+u_r) \tag{6b}$$

for the normal stress. Here Z_0 is the acoustic impedance of the liquid. The expression of the second member $u_y=a_nu_{ny}$ given in Eq. (6a) implies two assumptions. The first is that only the nth guided mode is excited by the incident wave. This situation is generally desirable in practice and can often be realized by choosing the incident angle according to the Snell's law and mode separation in the time domain (see also the discussion in the following section). Also the displacement associated with the excited mode given in Eq. (6a), when the liquid wedge is present, is assumed to be the same as that in the stress-free condition. This approximation is based on the approach of perturbation theory and is reasonable in most practical cases where the liquid density is much

smaller than that of the elastic waveguide.[21,22]

By the use of the boundary conditions of Eqs. (6), the substitution of T_{yy} $(y=b/2, z)$ into Eq. (2) leads to the mode amplitude equation written as

$$\left[\frac{d}{dz}+ik_n+\alpha_n\right]a_n(z)=-\frac{d\omega^2 Z_0 u_{ny}^*(b/2)u_i}{2P_n}, \tag{7}$$

where α_n is the attenuation per unit length of the guided wave in the presence of the liquid wedge and is given by

$$\alpha_n=d\omega^2\ Z_0|u_{ny}(b/2)|^2/(4P_n\ \cos\ \theta_n). \tag{8}$$

This attenuation physically stems from the energy leakage of the guided mode into the surrounding liquid during its propagation along the interface liquid–solid. If the second member is zero corresponding to the case where the incident wave is absent, Eq. (7) becomes homogeneous and the amplitude of $a_n(z)$ is proportional to $\exp(-\alpha_n z)$, which represents clearly a leaky mode traveling along the waveguide. According to Eq. (8), the greater the normal component of the excited mode, the greater the energy radiation into the liquid. The second member in Eq. (7) can be considered as an input force term due to the excitation by the incident wave. Like the attenuation coefficient α, this input force provided by the incident wave is also proportional to the normal component of the mode to be excited. This is because of the mechanical coupling via the normal stress between the incident (and radiated) wave and the waveguide.

Let us now find out the solution of the amplitude equation (7) when the incident beam is uniform and parallel. As shown in Fig. 1, the incident wave u_i is assumed constant and bounded between $z=0$ and $L=w/\cos\ \theta_n$ along the waveguide. The incident angle is chosen to verify Snell's law $k_n=k_0\ \sin\ \theta_n$, exciting the given mode cumulatively. The solution of the inhomogeneous equation (7) is the superposition of that of the homogeneous equation and a particular one. With the initial condition $a_n=0$ at $z=0$, the amplitude of the excited mode in the presence of the liquid wedge can be readily found as

$$a_n(z)=-a_i\ \exp(-ik_n z)[1-\exp(-\alpha_n z)](2/\alpha_n P_n)^{1/2}, \tag{9}$$

where $a_i=i\omega U_i(dZ_0\ \cos\ \theta_n/2)^{1/2}$ and U_i is the displacement amplitude of the incident wave. The amplitude of the excited mode leaving the liquid wedge is thus equal to the value of a_n taken at $z=L$. This amplitude will be constant during its propagation if lateral wave diffraction and material absorption are neglected. Substituting α_n of Eq. (8) into Eq. (9) yields the amplitude of the surface displacement of the excited mode $U_{ny}=a_n u_{ny}$ $(y=b/2)$, when normalized to the particle displacement U_i of the incident wave, as

$$U_{ny}/U_i=-2\ \cos\ \theta_n[1-\exp(-\alpha_n L)]. \tag{10}$$

This relationship is practical and can be easily verified by the experiment (see the next section). Equation (10) shows that the amplitude of the excited mode strongly depends on the parameter $h_n=\alpha_n L$, related to the wave leakage into the liquid in a reverse process to the excitation by an incident wave. It is noted that the displacement of the excited mode increases rapidly with $(\alpha_n L)$ and then remains nearly constant. Such ''saturation'' regions, already observed in the previous experiment (Fig. 41 of Ref. 1), confirm well this prediction. It implies that beyond certain values of L, the supplement of the incident power is totally utilized to balance the radiation into the liquid. To the contrary, without the inclusion of the reflected field $(u_r=0)$ and consequently the leaky loss $(\alpha_n=0)$, the surface displacement of the excited mode resolved from the mode amplitude equation, for $z=L$, is found as

$$U_{ny}=-U_i[d\omega^2 Z_0|u_{ny}(b/2)|^2/4P_n]L, \tag{11}$$

which is, except for notation, identical to the results given by previous theories.[1,26] Unlike Eq. (10), formula (11) predicts a linear dependence of the excited displacement on the width of the incident beam L. This divergent result, when increasing L, does not obviously agree with the experimental observation mentioned above. Moreover, the inclusion of the reflected field provides also the possibility to study[27] the nonspecular reflection phenomena, occurring when a bounded wave is incident on a layer at critical angles $\theta_n=\arcsin(c_0/v_n)$.[28]

To determine the performance of the wedge transducer it is necessary to calculate the efficiency function η_n, defined as the ratio of excited mode power to incident power and given by[23,24]

$$\eta_n=2[1-\exp(\alpha_n L)]^{1/2}/(\alpha_n L). \tag{12}$$

Thus the conversion efficiency is expressed in terms of a single parameter $h_n=\alpha_n L$, attaining a maximum value of 82% at $h=1.3$. In this specific waveguide where the surface wave is nondispersive $v_n=v_R$ (constant),[23,24] the efficiency η_R as a function of $h_R=\alpha_R L$ represents nothing else than efficiency vs frequency plot because the leak rate of the Rayleigh wave α_R is proportional to frequency.[21] As will be seen in the following section, the situation becomes much more complicated in other waveguides such as an elastic plate where multiple and dispersive modes coexist. As a result, the efficiency depends not only on frequency but also on geometry parameters of the waveguide and the transducer. Numerical calculations are often necessary to determine these material and geometry parameters required for optimum efficiency.

C. Numerical computation of Lamb waves excited in a plate waveguide

Lamb waves are the eigenmodes propagating in an elastic plate with stress-free boundary conditions $T_{22}=T_{12}=0$ at the two surfaces $y=\pm b/2$ (Fig. 1). Associated particle displacements are located in the sagittal plane formed by the direction of propagation and the axis normal to the plate plane. According to the symmetry of particle displacements with respect to the middle plane of the plate, the Lamb waves can be classified either as symmetric modes or as antisymmetric modes. Figure 2 displays the plots of phase velocity versus product fb (frequency×plate thickness) for the first few Lamb modes in an aluminium plate. Since the phase velocities are generally frequency dependent, the Lamb modes are dispersive. Among multiple Lamb modes, the lowest symmetric S_0 and antisymmetric A_0 Lamb modes

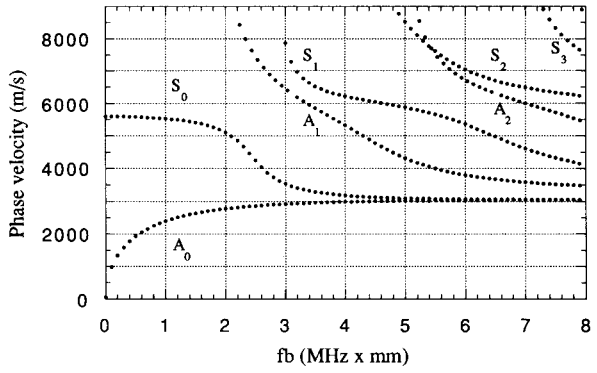

FIG. 2. Phase velocities of Lamb modes versus fb (product frequency-thickness) in an aluminium plate (v_1=6290 m/s and v_s=3280 m/s).

are of particular interest. They are qualitatively different from all other modes and can exist for any value of fb, whereas other high-order modes have cutoff frequencies. In the limit of $fb \gg 1$, both the S_0 and A_0 modes become asymptotic and approach to the velocity of Rayleigh wave.

Exciting a Lamb mode by the wedge method is to select the incident angle verifying the Snell law $\sin\theta_n = c_0/v_n$. The corresponding Lamb angles θ_n can be determined from the phase velocity shown in Fig. 2 as a function of the product fb. As mentioned in the preceding section, the mode amplitude as well as the efficiency function depend strongly on the leak rate of α_n into the liquid wedge [Eqs. (10) and (12)]. To determine α_n it is necessary, according to Eq. (8), to calculate the normal component of displacement at the plate surface normalized to $\sqrt{P_n}$. The power flow P_n defined by Eq. (3) is expressed in terms of stress and displacements, which can also be determined from the energy density and the group velocity V_g. For the nth guided mode, the average power flow takes the form[17,21]

$$P_n = \frac{1}{2}\rho\omega^2 (V_g)_n \int_{-b/2}^{b/2} (|u_{ny}|^2 + |u_{nz}|^2)\, dy, \tag{13}$$

which avoids laborious calculations of the stress field required in Eq. (3). Using Eq. (13), it is possible to calculate α_n from the particle displacement of the given mode alone.

Figure 3(a) and (b) shows the attenuation curves α versus the product fb for the two fundamental S_0 and A_0 modes for two different thicknesses b. It is found that, for a given value of fb, the leak rate α is inversely proportional to the plate thickness. Similar curves were presented previously by Merkulov,[29] who has resolved mathematically the characteristic equation, in a first-order approximation, of a plate immersed in a surrounding liquid. In comparison with that work, the present analysis has the advantage of giving a physical feel to the phenomena and establishing explicitly the relationship between the attenuation due to the wave radiation and the normal component of the displacement normalized to the power flow. It is seen in Fig. 3(a) that α starts from zero with the frequency, reaches a maximum value at $fb \approx 2.6$ MHz×mm, and increases asymptotically with f^2 when fb tends to infinity. In the limit as $fb \to 0$, the symmetrical mode S_0 behaves basically as a longitudinal wave with the displacement parallel to the plate surface, which

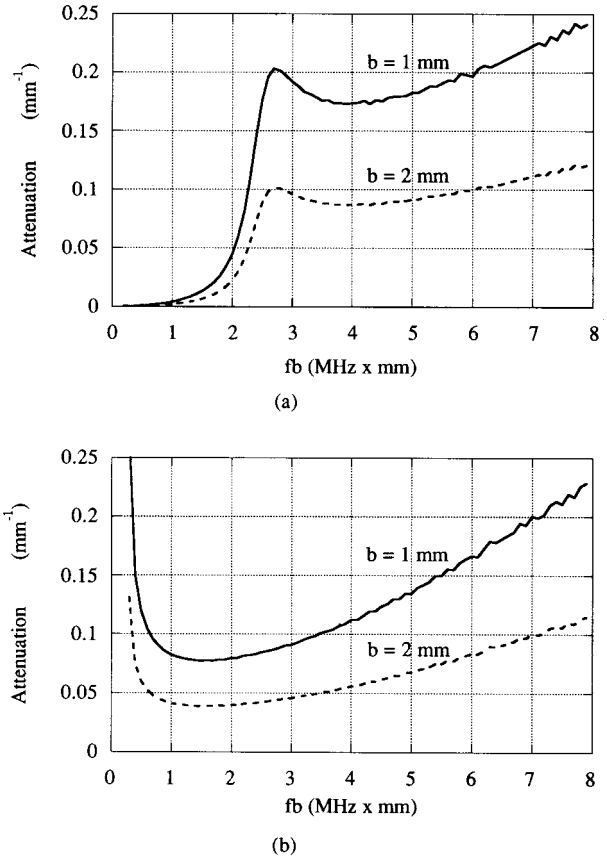

FIG. 3. Attenuation coefficients of Lamb modes S_0 (a) and A_0 (b) for two different thickness of plate b=1 and 2 mm, immersed in water.

explains the weak wave radiation (i.e., attenuation). When the frequency or the plate thickness becomes great ($fb \gg 1$), the S_0 mode is essentially concentrated at the surfaces of the plate. The radiation behavior into the surrounding liquid is thus the same as the Rayleigh wave which is proportional to f^2.[21] As shown in Fig. 3(b), the antisymmetrical A_0 mode behaves in the same way as the mode S_0 in the limit as $fb \to \infty$. To the contrary, the A_0 mode has an important radiation (and attenuation) in the low fb limit, caused by its flexural motion normal to the plate surface. The cutoff of the attenuation curves at $fb \approx 0.22$ MHz×mm is because the phase velocities of the A_0 mode below this limit are smaller than the sound velocity in the wedge liquid. As a result, no radiation of guided waves is allowed by the Snell law.

Now we search for the amplitudes of Lamb modes excited by the wedge method. By making use of the dispersion and attenuation results illustrated in Figs. 2 and 3, we carried out the numerical calculations directly from Eq. (10). Figure 4(a) and (b) show the surface displacements versus the product fb for the symmetrical S_0 mode excited in plates of thickness b=1 and 2 mm, respectively, by the wedge transducers of different sizes. As expected, the S_0 mode is hardly excited at the low-frequency limit because of the lack of the normal component of displacement coupling with the incident wave. After undergoing a rapid increase with the frequency, the amplitude of the S_0 mode attains a maximum value and remains rather constant over a wide frequency range. The displacements excited by the same transducers of

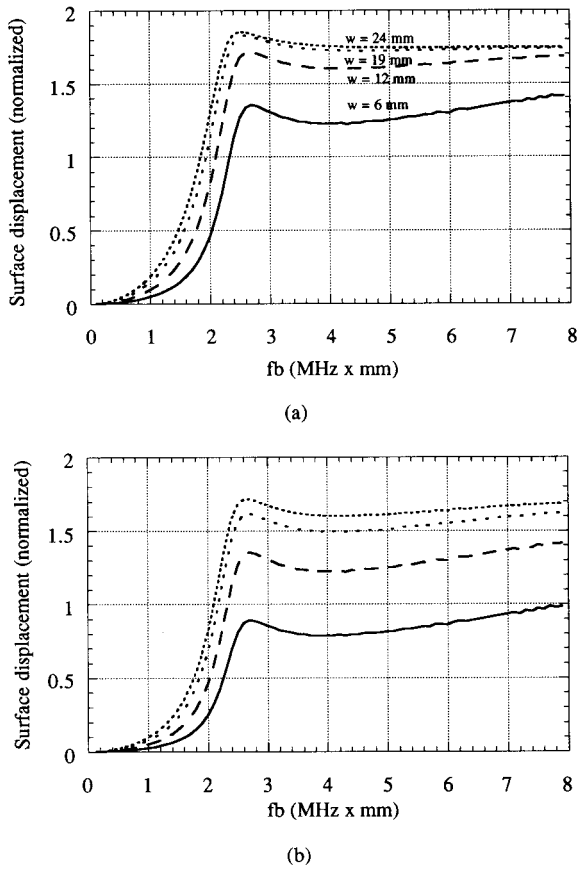

FIG. 4. Normalized surface displacement of S_0 mode in a 1-mm (a) and 2-mm (b) thick plates, excited by different sizes w of transducer.

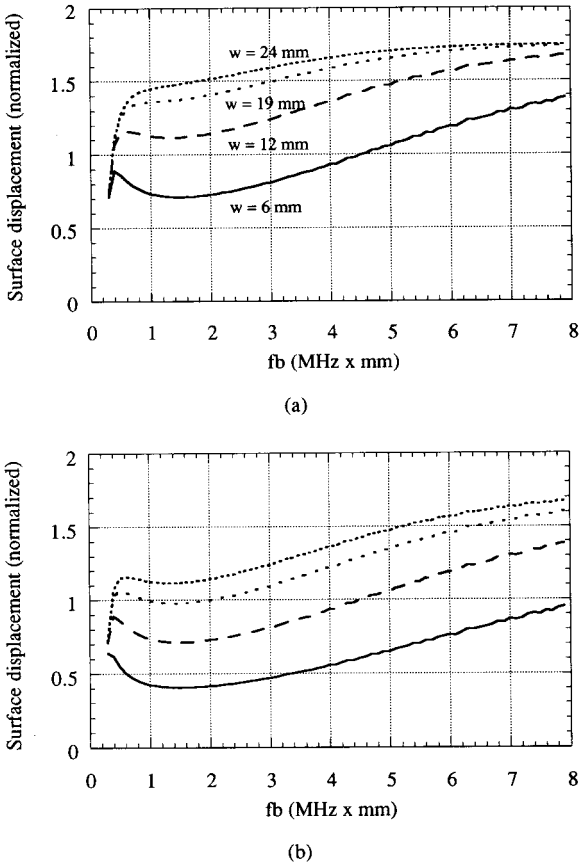

FIG. 5. Normalized surface displacement of A_0 mode in a 1-mm (a) and 2-mm (b) thick plates, excited by different sizes w of transducer.

the antisymmetrical A_0 mode are shown in Fig. 5. Compared to the S_0 mode, there is no abrupt variation although the amplitude of the A_0 mode increases a little with the frequency. For a given value of fb, the excited displacements of both the S_0 and A_0 modes are function of the plate thickness b. Besides, it is seen in Figs. 4 and 5 that the amplitude of the excited displacement increases, for a given frequency, with the size w of the transducer, i.e., the width of the incident beam. One possible explanation is that the Lamb waves are excited by an incident beam verifying the Snell's law. As the source is coherent, the larger the excitation zone, the greater the amplitude of the excited mode.

For a given amplitude of the incident wave U_i, increasing the beam width w implies an increase in the power supplied to the transducer. To appreciate the performance of a wedge transducer, it is useful to calculate its conversion efficiency η. Figures 6 and 7 present the efficiency functions obtained from Eq. (12) for the S_0 and A_0 modes, respectively. Maximum efficiencies of about 80% are attainable. In contrast to the Rayleigh wave where an ideal size of transducer $L=1.3/\alpha_R(f)$ exists at a given frequency for a maximum efficiency, the conditions required for optimum efficiency of Lamb waves are not so simple to determine. Indeed, the efficiency functions depend not only on frequency and transducer size, but also on the plate thickness and type of the modes to be excited.

II. EXPERIMENTS

To verify the above modal analysis of the Lamb excitation, we have made use of an experimental setup shown in Fig. 8. The wedge transducer is realized with a piezoelectric transducer immersed in a distilled water tank, which is in contact with an aluminum plate at the bottom across a thin plastic film ($\leqslant 10$ μm). The transducer is aligned so that the emitted beam strikes the boundary separating the water-loaded and the stress-free parts of the plate. The excited Lamb waves after leaving the liquid wedge propagate along a stress-free plate where the energy leakage into air is negligible. For a given incident beam, the normal displacement of the excited Lamb waves is detected at the polished plate surface using an optical heterodyne interferometer.[30] This displacement interferometer having a sensitivity of 10^{-4} Å/$\sqrt{\text{Hz}}$ is calibrated to 10 mV/Å. Detailed description of optical displacement or velocity interferometers operating at a reflecting or scattering surfaces can be found elsewhere.[15] As described below, the amplitude of the incident beam is also determined optically using an original interferometric method. The ratio of the excited displacement amplitude to the incident one will then permit a direct comparison with the theoretical value computed from Eq. (12). In previous experiments, the efficiency function[24] and the excited mode amplitude[31] were determined by measuring the round-trip insertion loss of the guided wave reflected from the edge of the waveguide. The present optical method presents an advan-

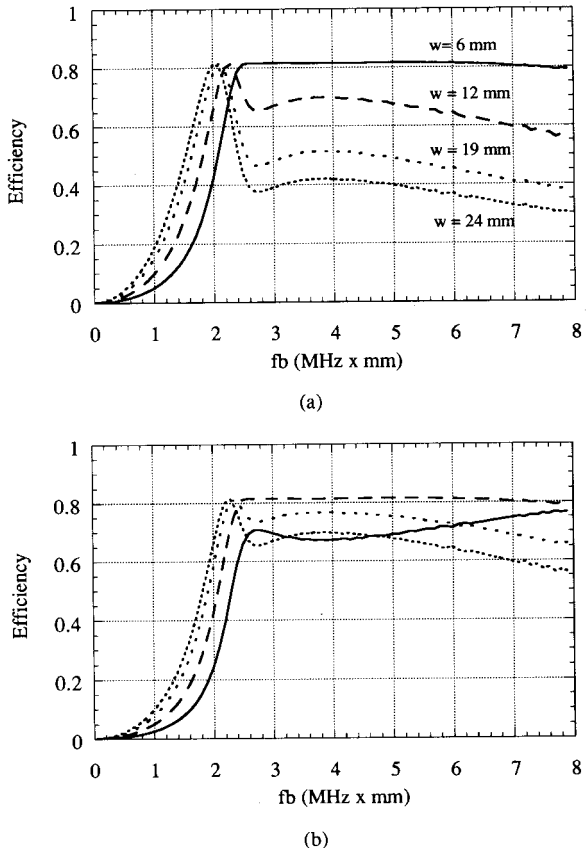

FIG. 6. Efficiencies for different sizes of transducer of generating the mode S_0 in 1-mm (a) and 2-mm (b) thick aluminium plates, respectively.

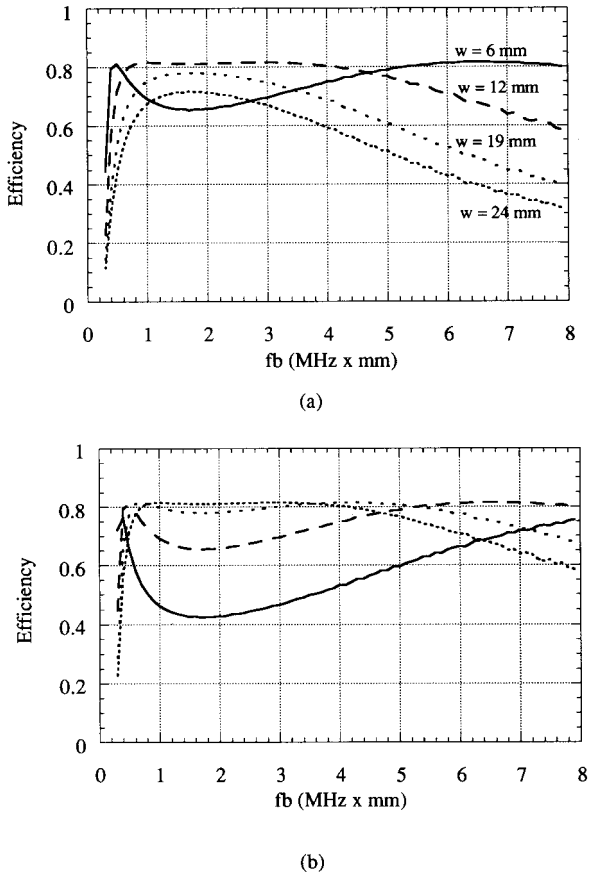

FIG. 7. Efficiencies for different sizes of transducer of generating the mode A_0 in 1-mm (a) and 2-mm (b) thick aluminium plates, respectively.

tage in being more direct and quantitative, avoiding the complicated process of mode conversion which may be encountered at the end of a plate waveguide.[11]

A. Determination of the incident wave amplitude

In the preceding section, the displacement of the excited Lamb mode is calculated as function of the incident wave. To compare with the theory, we need to determine experimentally the displacement amplitude associated with the incident wave striking the plate via liquid wedge. For doing this, an acousto-optic method combined with heterodyning detection was employed. This method, recently developed by the authors,[32–34] allows the acoustic pressure or dilatation to be measured inside a transparent medium. As shown by the schematic diagram in Fig. 9(a), a laser probe beam crossing normally an acoustic wave undergoes an optical phase shift due to the acousto-optic effect, $\Delta\phi(t)=(2\pi\mu/\lambda)p(t)d$. Here μ is the photoelastic constant of fluid media, $p(t)$ is the acoustic pressure, and d is the length of the acoustic beam. This probe beam is then mixed with a reference beam issuing from the same laser source. The signal resulting from the interference at the photodetector level will be $i(t)=(I_0/2)\cos[\omega_B t+\Delta\phi(t)]$, where I_0 is the laser intensity of the source and ω_B is the frequency shift of either the reference or probe beam produced by an acousto-optic modulator (heterodyning). This phase shift proportional to the acoustic pressure can be demodulated by a broadband electronic processing similar to that for displacement measurement.[30] Figure 9(b) shows a typical pressure toneburst of an incident beam, emitted by a Panametrics transducer of nominal diameter of 12 mm. It is driven at 2 MHz by HP 8116A generator through an ENI A150 amplifier. The measured amplitude of pressure was 2.7 ± 0.15 atm. The corresponding particle displacement can be deduced readily by the relationship $u=p/(\omega Z_0)$, where Z_0 is the acoustic impedance of water and ω is the incident angular frequency. For example, the mean amplitude of the particle displacement deduced from the pressure shown in Fig. 9(b) is 14 nm.

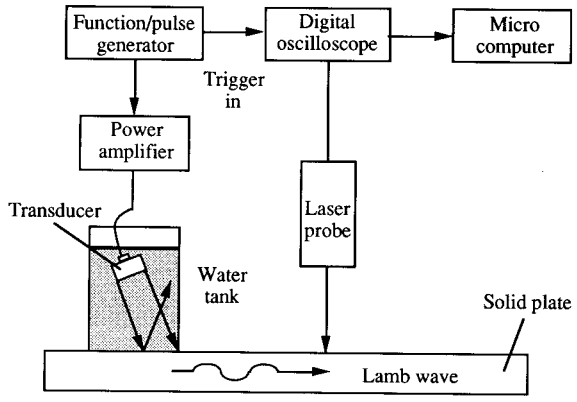

FIG. 8. Experimental arrangement for generating and detecting the Lamb waves in a plate.

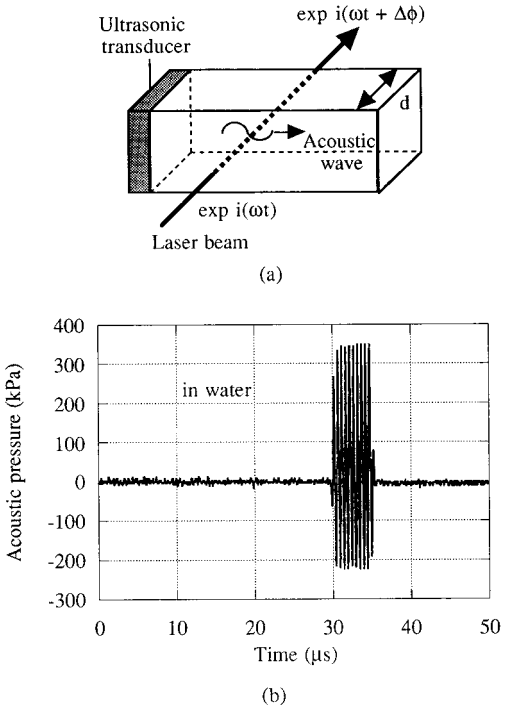

FIG. 9. (a) Schematic diagram of ultrasonic pressure detected by optical method; (b) longitudinal wave used to excite the Lamb modes through the water wedge is measured by an optical interferometric method.

B. Measurements of Lamb modes

A ten-cycle toneburst of longitudinal wave shown in Fig. 9(b) was used to excite Lamb modes in 1-mm-thick aluminum plate, placed in the far field of the transducer. In this work, our attention was focused on the observation of the two fundamental Lamb modes S_0 and A_0. In order to ease the interpretation of the received signal, the frequency of the toneburst varied so as to give a product of fb (frequency thickness) from 1–3 MHz×mm. In these regions of fb, only the fundamental S_0 and A_0 modes are dominant and propagate with different phase velocities. According to Snell's law $\sin\theta_n = c_0/v_n$, the two modes can be excited separately with different incident angles. When the frequency increases, the phase velocities of the S_0 and A_0 modes approach each other and the two modes can be excited at a given angle ($\theta \approx 30°$) due to the beam spreading of incident wave. It was not a problem in our experiment to isolate the mode of interest from the rest of the received signal, since the corresponding group velocities are different, causing mode separation in the time domain. In the present case where the incident beam is large compared to the wavelength, the maximum amplitude of a given Lamb mode is achieved when the incident angle is chosen according to the Snell's law.[1,26] Varying the incident angle θ as function of fb allows us to generate Lamb modes with different wavelength as shown in Fig. 2.

Typical displacement waveforms measured by optical interferometer of the Lamb modes S_0 and A_0 are displayed in Fig. 10. They were generated with a center frequency thickness of $fb = 2$ MHz×mm at an incident angle of 19° and 34°, respectively. The phase velocities deduced from Snell's law, with sound velocity $c_0 = 1500$ m/s in water, were 4600 and

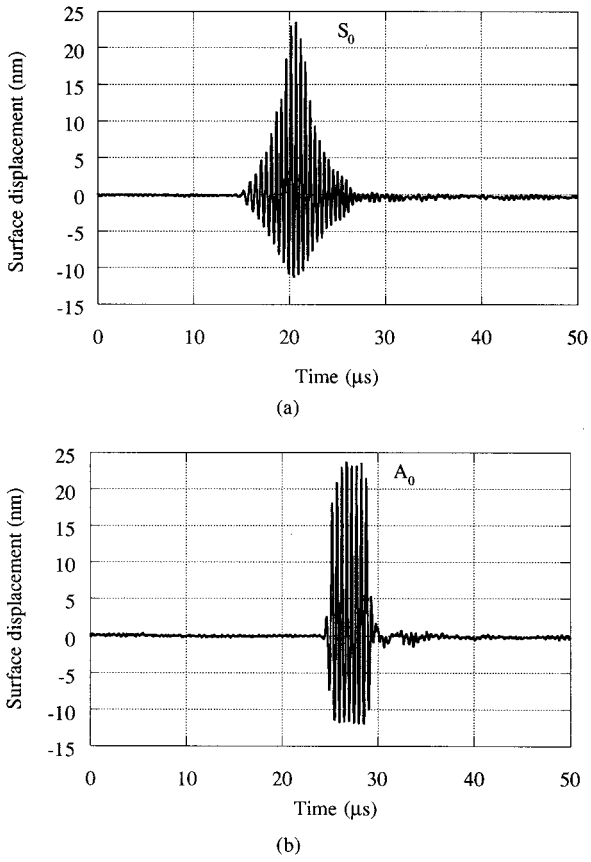

FIG. 10. Typical displacement waveforms of the excited Lamb modes S_0 (a) and A_0 (b) in a 1-mm-thick aluminium plate.

2680 m/s, corresponding well to those predicted by the theoretical dispersion curves (Fig. 2). Unlike mode A_0, the waveform of mode S_0 was distorted in comparison with that of the incident wave. This distortion arose probably from the rapid variation of its displacement response at this frequency range [Fig. 4(a)]. The peak-to-peak amplitudes of the S_0 and A_0 modes were measured for different frequency of excitation. The frequency increment in each case was 0.1 MHz. Figure 11 shows the measured amplitudes normalized to the incident wave versus the product fb, along with the theoretical curves. Overall, there is a qualitative agreement between theory and experiment both for order and frequency dependence. Several observations can be made concerning the discrepancy between the theoretical and the experimental results. First, as in the previous studies,[23,24,26] two-dimensional striplike sources were assumed in the present theory whereas the transducer used in the experiment was of circular nature. Second, the theoretical assumption of a uniform incident beam was different from the practical one generally in Gaussian form.[31] Also the beam spreading effects neglected in the theory but present in the experiment can induce error for determining effective incident beam (transducer) size.

III. CONCLUSION

A modal analysis is developed for determining the amplitudes of Lamb waves generated by a parallel and uniform incident longitudinal wave. Using a perturbation theory, the reflected wave contribution as well as the Lamb wave leak-

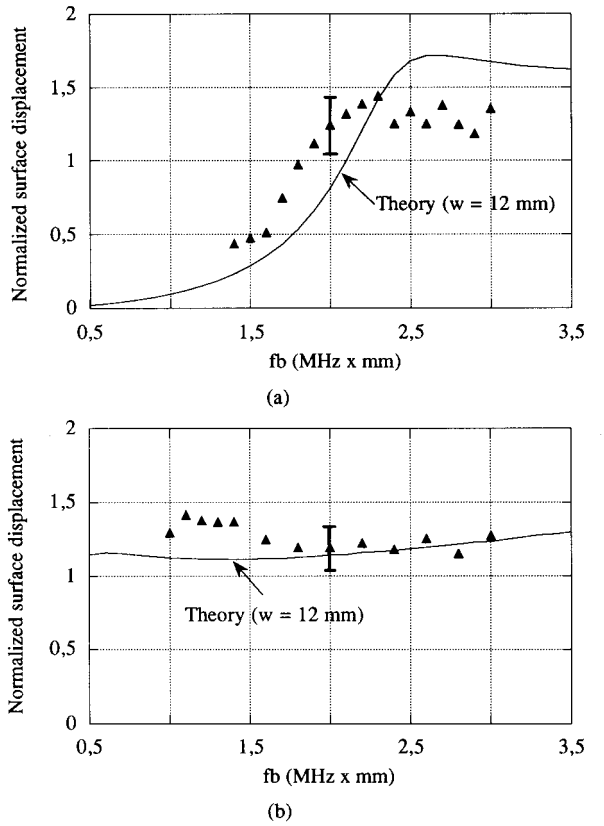

FIG. 11. Comparison between the theoretically predicted and experimental obtained (triangle dots) surface displacements for the modes S_0 (a) and A_0 (b). Experimental uncertainties are indicated by typical error bars.

age have been accounted for in the theory to give an analytical expression of the excited displacement. Numerical calculations have been performed for the two fundamental Lamb modes S_0 and A_0 propagating in 1- and 2-mm-thick aluminum plates, respectively. The theoretical results showed that, in addition to the thickness of the plate, the excited Lamb wave displacements and the efficiency function depend on the frequency and also the width of the incident beam. Owing to the optical interferometric method, the normalized surface displacement of excited S_0 and A_0 modes have been measured in a 1-mm-thick aluminum plate. These preliminary results confirmed quite well the theoretical prediction. In future work, we will improve the present theory by considering an inhomogenous such as Gaussian incident beam and conduct the experiments with well-defined acoustic beams emitted by striplike (two-dimensional) transducers.

ACKNOWLEDGMENTS

The author is grateful to Professors B. Auld and G. Quentin for the helpful discussions and also thanks the reviewers for the critical reading of the manuscript.

[1] I. A. Victorov, *Rayleigh and Lamb Waves* (Plenum, New York, 1967).
[2] S. I. Rokhlin, ''Lamb wave interaction with lap-shear adhensive joint: Theory and experiment,'' J. Acoust. Soc. Am. **89**, 2758–2765 (1991).
[3] D. N. Alleyne and P. Cawley, ''The interaction of Lamb waves with defects,'' IEEE Trans. Ultrason. Ferroelectr. Freq. Control **UFFC-39**, 381–397 (1992).
[4] A. H. Nayfeh and D. E. Chimenti, ''Propagation of guided waves in fluid-coupled plates of fiber-reinforced composites,'' J. Acoust. Soc. Am. **83**, 1736–1743 (1988).
[5] V. Dayal and V. K. Kinra, ''Leaky Lamb waves in an anisotropic plate. I: An exacte solution and experiments,'' J. Acoust. Soc. Am. **85**, 2268–2276 (1989).
[6] D. A. Hutchins and K. Lundgren, ''A laser study of transient Lamb waves in thin materials,'' J. Acoust. Soc. Am. **85**, 1441–1448 (1989).
[7] S. W. Wenzel and R. M. White, ''A multisensor employing an ultrasonic Lamb wave oscillator,''IEEE Trans. Electron Devices **ED-35**, 735–743 (1988).
[8] Y. Jin and S. G. Joshi, ''Coupling of interdigital transducer to ultrasonic Lamb waves,'' Appl. Phys. Lett. **58**, 1830–1832 (1991).
[9] E. Dieulesaint, D. Royer, O. Legras, and A. Chaabi, ''Acoustic plate mode touch screen,'' Electron. Lett. **27**, 49–51 (1991).
[10] R. J. Dewhurst, C. Edwards, A. D. W. McKie, and S. B. Plamer, ''Estimation of the thickness of thin metal sheet using laser generated ultrasound,'' Appl. Phys. Lett. **51**, 1066–1068 (1987).
[11] C. F. Ying, ''Photoelastic visualization and theoretical analyses of scattering of ultrasonic pulses in solids,'' in *Physical Acoustics*, edited by R. N. Thurston (Academic, New York, 1990), Vol. 19, Chap. 7.
[12] R. B. Thompson, G. A. Alers, and M. A. Tennison, ''Application of direct electromagnetic Lamb wave generation to gas pipeline inspection,'' in *Proceedings of IEEE Ultrasonics Symposium* (IEEE, New York, 1972), pp. 91–94.
[13] W. M. D. Wright, D. W. Schindel, and D. W. Hutchins, ''Studies of laser-generated ultrasound using a micromachined silicon electrostatic transducer in air,'' J. Acoust. Soc. Am. **95**, 2567–2575 (1994).
[14] D. A. Hutchins, ''Ultrasonic generation by pulsed lasers,'' in *Physical Acoustics*, edited by W. P. Mason and R. N. Thurston (Academic, New York, 1988), Vol. 18, Chap. 1.
[15] C. B. Scruby and L. E. Drain, *Laser Ultrasonics—Techniques and Applications* (Hilger, Bristol, 1990).
[16] J. Miklowitz, *The Theory of Elastic Waves and Waveguides* (North-Holland, Amsterdam, 1978).
[17] J. D. Achenbach, *Wave Propagation in Eastic Solids* (North-Holland, Amsterdam, 1973).
[18] R. L. Weaver and Y. H. Pao, ''Axisymmetric elastic waves excited by a point source in a plate,'' J. Appl. Mech. **49**, 821–836 (1982).
[19] J. B. Spicer, A. D. W. McKie, and J. W. Wagner, ''Quantitative theory for laser ultrasonic waves in a thin plate,'' Appl. Phys. Lett. **57**, 1882–1884 (1990).
[20] V. V. Shevchenko, *Continous Transmission in Open Waveguides* (Golem, Boulder, CO, 1971).
[21] B. A. Auld, *Acoustic Felds and Waves in Solids* (Wiley, New York, 1973), Vol. 2.
[22] G. S. Kino, *Acoustic Waves: Devices, Imaging, and Analog Signal Processing* (Prentice-Hall, Englewood Cliffs, 1987).
[23] H. L. Bertoni and T. Tamir, ''Characteristics of wedge transducers for acoustic surface waves,'' IEEE Trans. Sonics Ultrason. **SU-22**, 415–420 (1975).
[24] J. Fraser, B. T. Khuri-Yakub, and G. S. Kino, ''The design of efficient broadband wedge transducers,'' Appl. Phys. Lett. **32**, 698–700 (1978).
[25] R. Briers, O. Leroy, and G. N. Shkerdin, ''Mode theory as a framework for the investigation of the generation of a Stoneley wave at liquid-solid interface,'' J. Acoust. Soc. Am. **95**, 1953–1966 (1994).
[26] J. J. Ditri and J. L. Rose, ''Excitation of guided waves in generally anisotropic layers using finite sources,'' J. Appl. Mech. **61**, 330–338 (1994).
[27] X. Jia, ''Normal-mode theory of nonspecular phenomena for a finite-aperture ultrasonic beam reflected from layered media,'' Appl. Phys. Lett. **70**(3), 309–311 (1997).
[28] H. L. Bertoni and T. Tamir, ''Unified theory of Rayleigh-angle phenomena for acoustic beams at liquid-solid interfaces,'' Appl. Phys. **2**, 157–172 (1973).
[29] L. G. Merkulov, ''Damping of Normal modes in a plate immersed in liquid,'' Sov. Phys. Acoust. **10**, 169–173 (1964).
[30] D. Royer and E. Dieulesaint, ''Optical detection of sub-angström transient mechanical displacements,'' in *Proceedings of IEEE Ultrasonics Symposium* (IEEE, New York, 1986), pp. 527–530.

[31] K. M. Rajana, D. Hongerholt, J. L. Rose, and J. J. Ditri, ''Analysis of the generation of guided waves using finite sources: an experimental approach,'' in *Review of Progress in Quantitative Nondestructive Evaluation, Vol. 14* (Plenum, New York, 1995), pp. 171–178.
[32] X. Jia, G. Quentin, and M. Lassoued, ''Optical heterodyne detection of pulsed ultrasonic pressures,'' IEEE Trans. Ultrason. Ferroelectr. Freq. Control **UFFC-40**, 67–69 (1993).
[33] X. Jia, A. Boumiz, and G. Quentin, ''Laser interferometric detection of ultrasonic waves propagating inside a transparent solid,'' Appl. Phys. Lett. **63**, 2192–2194 (1993).
[34] X. Jia, Ch. Mattei, and G. Quentin, ''Analysis of optical interferometric measurements of guided acoustic waves in transparent solid media,'' J. Appl. Phys. **77**, 5528–5537 (1995).